Inorganic Chemistry

pubs.acs.org/IC

Article

Isocyanide Substituent Influences Reductive Elimination versus Migratory Insertion in Reaction with an $[Fe_2(\mu\text{-}H)_2]^{2+}$ Complex

Titto Sunil John, Łukasz Dobrzycki, Vincent J. Catalano, and Leslie J. Murray*

Cite This: *Inorg. Chem.* 2024, 63, 21083−21091

Read Online

ACCESS | Metrics & More | Article Recommendations | Supporting Information

ABSTRACT: Iron hydrides are proposed reactive intermediates for N_2 and CO conversion in industrial and biological processes. Here, we report a reactivity study of a low-coordinate di(μ-hydrido)diiron(II) complex, $Fe_2(\mu\text{-}H)_2\mathbf{L}$, where $\mathbf{L}^{2-}$ is a bis(β-diketiminate) cyclophane, with isocyanides, which have electronic structures related to N_2 and CO. The reaction outcome is influenced by the isocyanide substituent, with 2,6-xylyl isocyanide leading to H_2 loss, to form a bis(μ-1,1-isocyanide)diiron(I) complex, whereas all of the other tested isocyanides insert into the Fe−H bond to give (μ-1,2-iminoformyl) complexes. Steric bulk of the isocyanide substituent determines the extent of insertion (i.e., into one or both Fe−H−Fe units) with *tert*-butyl isocyanide reacting to yield the mono-(μ-1,2-iminoformyl)diiron(II) complex, exclusively, and isopropyl- and methyl isocyanides affording the bis(μ-1,2-iminoformyl)diiron(II) products. Treatment of $Fe_2(\mu\text{-}1,2\text{-}CHNtBu)(\mu\text{-}H)\mathbf{L}$ with 2,6-xylyl isocyanide (or XylNC) yields $Fe_2(\mu\text{-}XylNC)_2\mathbf{L}$ and *tert*-butylaldimine as one of the organic products.

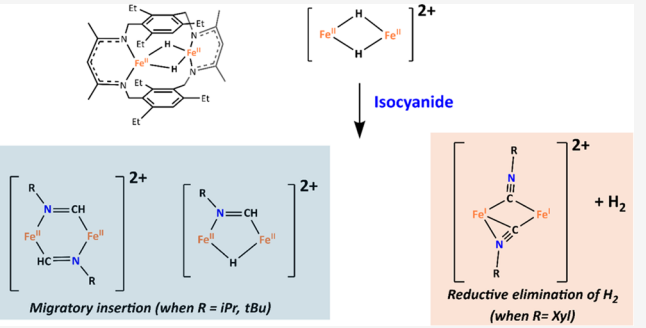

INTRODUCTION

Activation of dinitrogen and carbon monoxide remain active areas of chemical research, given relevance to biological and industrial N_2 fixation and the Fischer−Tropsch process, respectively. Metal hydrides are proposed as intermediates in these processes, with particular interest in the reactivity of iron hydrides as this metal is common to catalysts for both N_2 and CO activation. For example, proposed dissociative adsorption of H_2 and either N_2 or CO on catalyst surfaces for the Haber−Bosch or Fischer−Tropsch processes, respectively, lead to NH_3 or hydrocarbon formation.[1−3] In homogeneous systems, metal hydrides serve as a type of protecting group for low-valent metal centers as H_2 reductive elimination unmasks the reduced metal centers.[4−8] Isocyanides are a useful proxy for CO and N_2 for reactivity studies; these three molecules have a pair of accessible π-accepting orbitals, albeit with differences in the σ donor strength and π-acidity.[9] Unsurprisingly then, isocyanides are competent inhibitors or alternative substrates for N_2 in the catalytic systems noted above.[4,10,11] In contrast to N_2, the steric bulk of the isocyanide substituent provides an additional handle to limit the metal coordination number and stabilize structural analogues of proposed reactive intermediates otherwise inaccessible using CO or N_2.[12−15] Typically, isocyanides react with metal hydrides by migratory insertion into the M−H bond to yield iminoformyl (−C(H)NR) or aminocarbyne (−CN(H)R) complexes or by H_2 reductive elimination followed by isocyanide coordination in terminal or μ-1,1 modes depending on complex nuclearity.[16−20] Notably, Rosenberg and co-workers observed differences in the site of migratory insertion (viz. C or N) in the reaction of a triosmium dihydride cluster with isocyanides as a function of the isocyanide substituent,[21] and similar results were reported for $W_2(\mu\text{-}H)_2(CO)_4(\eta^5\text{-}Cp)_2$.[23] Comparable control of insertion vs reductive elimination can be afforded by tuning the steric demands of the ancillary ligands in dimanganese di(μ-hydride) complexes (Scheme 1).[22]

Previously, our group reported that a di(μ-hydrido)diiron complex, $Fe_2(\mu\text{-}H)_2\mathbf{L}$ ($\mathbf{L}^{2-}$ = bis(β-diketiminate)cyclophane), reacts with CO to reductively eliminate H_2 and yield a di(μ-carbonyl)diiron(II) complex, $Fe_2(\mu\text{-}CO)_2\mathbf{L}$ (Scheme 2).[24] Here, we extend that work toward reaction with isocyanides and observe a substituent-dependent reductive elimination of H_2 or migratory insertion. Varying the equivalents of isocyanide used or the substituent from methyl to *tert*-butyl results in the retention of one μ-hydride ligand to yield the (μ-hydrido)(μ−κC:κN-iminoformyl) diiron product instead of the bis(iminoformyl) diiron(II) complex observed for reaction with 2 equiv of methyl and isopropyl isocyanides. Reaction of $Fe_2(\mu\text{-}HCNtBu)(\mu\text{-}H)\mathbf{L}$ with xylyl isocyanide effects aldimine loss, and is a rare example of isocyanide to aldimine

Received: August 1, 2024
Revised: October 8, 2024
Accepted: October 16, 2024
Published: October 24, 2024

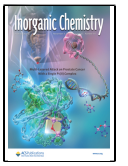

https://doi.org/10.1021/acs.inorgchem.4c03256
Inorg. Chem. 2024, 63, 21083−21091

Scheme 1. Prior Reports of Reactivity of Polynuclear Transition-Metal Hydrides with Isocyanides Demonstrating Dependence on the Isocyanide Substituent or the Ancillary Ligand

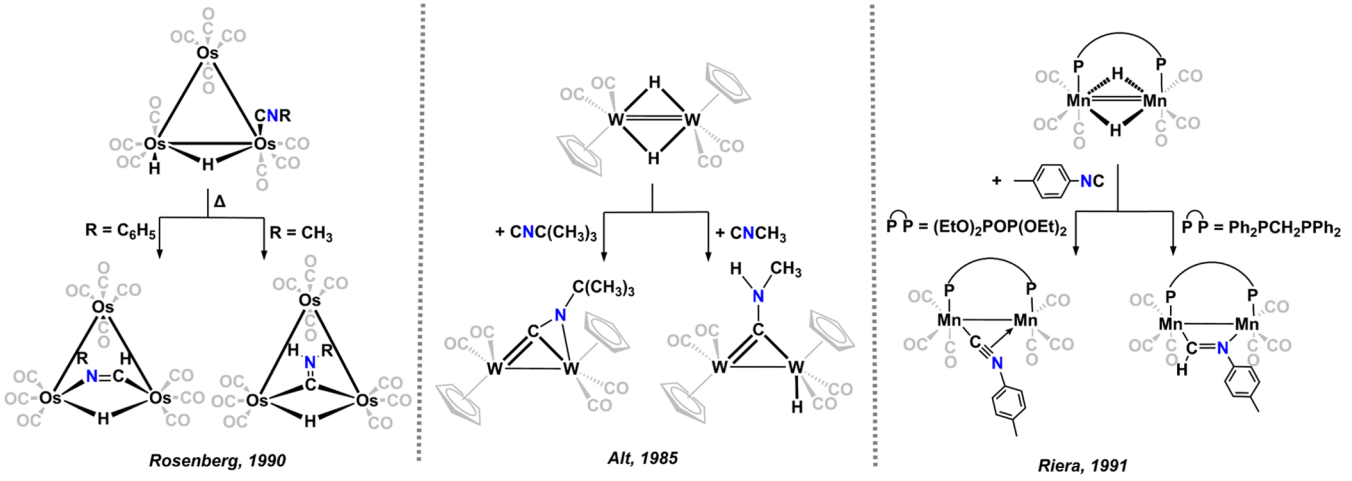

Scheme 2. Synthesis of the Reported Complexes from $Fe_2(\mu\text{-}H)_2L$ by Treatment with Isocyanides[a]

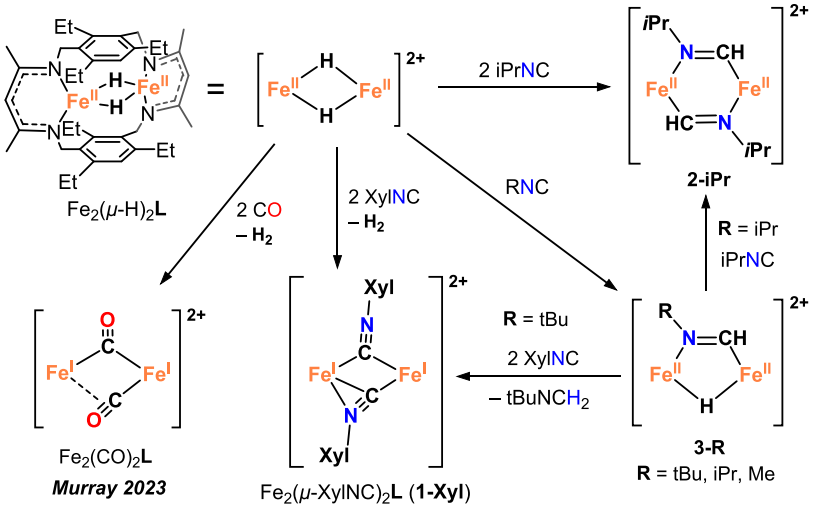

[a]Complexes are abbreviated as the diiron core with L^{2-} omitted for clarity.

conversion.[12] The substituent control over the extent of insertion as well as over reductive elimination observed here is distinct from the precedent.

EXPERIMENTAL METHODS

General Considerations. All manipulations were performed within an Ar-filled Vigor glovebox, unless otherwise stated. Tetrahydrofuran (THF), benzene, toluene, *n*-hexane, and diethyl ether were purchased from Sigma-Aldrich, dried using an Innovative Technologies solvent purification system (now Inert, Amesbury, MA), transferred to the glovebox, and stored over activated 3 Å molecular sieves (200 °C, <20 mT) for at least 24 h prior to use, with water contents below 25 ppm determined using a Mettler Toledo C20 Coulometric Karl Fischer titrator. C_6D_6 was purchased from Cambridge Isotope Laboratories, dried at reflux over CaH_2, then distilled, degassed, transferred to the glovebox, and stored over activated 3 Å molecular sieves. 2,6-Dimethylphenyl-, phenyl-, *tert*-butyl-, and isopropyl-isocyanides were purchased from Oakwood Chemical (Estill, SC). Methyl isocyanide and $Fe_2(\mu\text{-}H)_2L$ were prepared as reported elsewhere.[24,25] ^{1}H nuclear magnetic resonance (^{1}H NMR) spectra were recorded on a Bruker 400 MHz spectrometer or an Inova 500 MHz equipped with a three-channel indirect detection probe with *z*-axis gradients. ^{1}H NMR spectra of paramagnetic complexes were collected with a 0 s relaxation delay, an acquisition time of 0.3 s, and 256 scans. ^{1}H NMR spectra of organic diamagnetic products were collected using a 1.0 s relaxation delay and a 3.6 s acquisition time and averaged over 16 scans. Chemical shifts were reported in δ (ppm) and were referenced to residual internal C_6D_5H resonance at δ_H = 7.16 ppm for benzene-d_6. Fourier-transform infrared (FT-IR) spectra were collected on drop-cast samples using a ThermoFisher Scientific Nicolet iS5 spectrometer with an iD7 ATR stage operated by the OMNIC software package with a resolution of 1.0 cm^{-1} and 32 scans per sample. Mass spectrometry data were collected on an Agilent 6230 ESI-TOF for which the flow lines were extensively rinsed with anhydrous air-free THF prior to use, in positive mode by direct injection of samples as anhydrous THF solutions, and with a gas temperature and a fragmentation voltage of 350 °C and 125.0 V, respectively.

X-ray Crystallography. Low-temperature X-ray diffraction data for **1-Xyl**, **2-iPr**, and **3-tBu** were collected on a Rigaku XtaLAB Synergy diffractometer coupled to a Rigaku Hypix detector using Cu Kα radiation (λ = 1.54184 Å) from a PhotonJet microfocus X-ray source at 100 K. The diffraction images were processed and scaled using the CrysAlisPro software.[26] The structures were solved through intrinsic phasing using SHELXT and refined against F^2 on all data by full-matrix least-squares with SHELXL following established refinement strategies.[27−29] All nonhydrogen atoms were refined anisotropi-

https://doi.org/10.1021/acs.inorgchem.4c03256
Inorg. Chem. 2024, 63, 21083−21091

cally. All hydrogen atoms bound to carbon were included in the model at geometrically calculated positions and refined by using a riding model. The isotropic displacement parameters of all hydrogen atoms were fixed to 1.2 times the U_{eq} value of the atoms they are linked to (1.5 times for methyl groups). In the structure of **3-tBu**, the *t*-butyl group and one ethyl group of the arene cap in the $\mathbf{L}^{2-}$ ancillary ligand are disordered over two sites with refined occupancy yielding 0.587(5):0.413(5) and 0.55(3):0.45(3), respectively (Figure S26). To preserve the reasonable geometry of disordered fragments, various distance and angle restraints were used. Details of the data quality and a summary of the residual values of refinements are listed in Tables S2, S3, and S5 for **1-Xyl**, **2-iPr**, and **3-tBu**, respectively.

X-ray measurements of **3-iPr** and **3-Me** were performed at 100(1) and 180(1) K, respectively, on a BRUKER D8 Venture with a PHOTON III four-circle diffractometer system equipped with a INCOATEC IμS 3.0 microfocus X-ray tube (Mo Kα, λ = 0.71073 Å) and a HELIOS multilayer optics monochromator. Frames were collected with a Bruker APEX3 program.[30] The frames were integrated with the Bruker SAINT software package using a narrow-frame algorithm.[31] Data were corrected for absorption effects using the Multi-Scan method (SADABS).[32] The structure of **3-iPr** was solved through the intrinsic phasing method and refined using the Bruker SHELXTL software package.[28,33] The structure is disordered with part of the molecule including the phenyl moiety with substituents distributed over two positions with a refined occupancy ratio yielding 0.565(6):0.435(6) (Figure S26). A number of distance and angle restraints were used to preserve reasonable geometry of disordered fragments. All nonhydrogen atoms (including disordered groups) were refined anisotropically with applied restraints for modeling ADPs of some disordered atoms. All hydrogen atoms, except the hydride ligand, were placed in calculated positions and refined within the riding model. Coordinates and temperature factor of the hydride ligand are fully refined. Temperature factors of all C-bound H atoms were not refined and were set to be either 1.2 or 1.5 times larger than the U_{eq} of the corresponding heavy atom. Details of the data quality and a summary of the residual values of the refinements are given in Table S4. The structure of **3-Me** was solved through a direct method using the Bruker SHELXTL software package.[28,33] The structure is disordered with part of the molecule, including one Fe site, one phenyl moiety with substituents, and the coordinated imine, distributed over two positions with a refined occupancy ratio of 0.576(14):0.424(14) (Figure S26). As for prior structure solutions, distance and angle restraints were employed to preserve a reasonable geometry of the disordered fragment. All nonhydrogen atoms (including disordered groups) were refined anisotropically with applied restraints for modeling ADPs of some disordered atoms. All hydrogen atoms, except for hydride, were placed in calculated positions and refined within the riding model. The hydride ligand coordinated to the Fe centers is disordered over three positions and located between the heavy atoms. Coordinates of the disordered hydride ligands are refined with Fe−H distance restraints. Temperature factors of all H atoms were not refined and were set to be either 1.2 or 1.5 times larger than U_{eq} of the corresponding heavy atom. Details of the data quality and a summary of the residual values of the refinements are listed in Table S6.

$Fe_2(\mu$-XylNC)$_2$L, 1-Xyl. To a solution of $Fe_2(\mu\text{-H})_2\mathbf{L}$ (50.0 mg in PhMe, 73.4 μmol) stirred with a Pyrex-coated magnetic stir bar was added 2,6-xylyl isocyanide (20.2 mg in 2 mL of PhMe, 154 μmol) dropwise. The reaction was stirred at ambient temperature for 3 h over which the reaction mixture gradually changed from dark brown to reddish-brown. The solvent was removed under reduced pressure to afford **1-Xyl** as a dark red solid (57.6 mg, 83.4%). Single crystals suitable for X-ray diffraction were grown by cooling a saturated solution of as-isolated **1-Xyl** in PhMe to −33 °C for 2 days to afford dark brown crystals (8.0 mg, 12.6%). The solution was saturated at 60 °C and filtered through a Celite plug, which was prerinsed with anhydrous PhMe. ^{1}H NMR (400 MHz, C_6D_6, 298 K) δ (ppm): 101.47, 24.43, 6.96−7.39, 2.11, 2.01, 0.27, −40.20, −45.16, −80.54, and −90.41. ATR-IR (cm^{-1}): 2960, 2925, 2867, 1854, 1820, 1605, 1563, 1525, 1460, 1428, 1399, 1372, 1328, 1012, 763. Anal. Calcd. for $C_{56}H_{72}N_6Fe_2$·0.4 THF (%): C, 71.49; H, 7.71; N, 8.93. Found: C, 70.97; H, 7.90; N, 8.49. μ_{eff} = 6.9(2) μ_B.

$Fe_2(\mu$−κC:κN-HCNiPr)$_2$L, 2-iPr. $Fe_2(\mu\text{-H})_2\mathbf{L}$ (50.0 mg, 73.4 μmol) was dissolved in 4 mL of PhMe taken in a 20 mL scintillation vial. The sample was stirred using a PTFE stir bar and cooled to −33 °C. To this sample, 1.5420 mL of a 0.1 M stock solution of iPrNC in PhMe precooled to −33 °C was added dropwise. The resulting dark red solution was stirred for 12 h at ambient temperature. Volatiles were removed under reduced pressure to yield **2-iPr** as a dark brown solid (49.6 mg, 83.1%). Single crystals suitable for X-ray diffraction analysis were grown by layering hexanes on a saturated PhMe solution of **2-iPr** at −33 °C for 2 days (8.0 mg, 13.3%). The PhMe solution was saturated by heating to 60 °C briefly (<30 s) and then filtered through a Celite plug, which was prerinsed with anhydrous PhMe. ^{1}H NMR (400 MHz, C_6D_6, 298 K) δ (ppm): 82.94, 70.54, 58.19, 54.54, 4.22, 2.12, 0.83, 0.31, 0.30, −2.22, −9.61, −20.74, −22.18, −26.15, −28.15. ATR-IR (cm^{-1}): 2960, 2925, 2868, 1515, 1466, 1429, 1397, 1372, 1325, 1016. Anal. Calcd. for $C_{46}H_{70}N_6Fe_2$ (%): C, 67.47; H, 8.62; N, 10.26. Found: C, 67.20; H, 8.23; N, 9.16. μ_{eff} = 5.7(2) μ_B.

$Fe_2(\mu$−κC:κN-HCNiPr)(μ-H)L, 3-iPr. $Fe_2(\mu\text{-H})_2\mathbf{L}$ (10.0 mg, 14.6 μmol) was added to a 20 mL scintillation vial containing a Teflon magnetic stir bar and 4.0 mL of PhMe, and the solution was cooled to −33 °C. To this solution was added iPrNC in PhMe (147.0 μL, 0.1 M solution, 14.7 μmol) cooled to −33 °C dropwise and stirred at ambient temperature for 12 h. The solvent was then removed under reduced pressure to afford a brownish-red solid (10.1 mg, 91.0%). Single crystals suitable for X-ray diffraction were obtained by the dissolution of the brownish-red solid in benzene (70 °C), followed by the slow evaporation of the solvent into mineral oil at ambient temperature after 7 d. ^{1}H NMR (400 MHz, C_6D_6, 298 K) δ (ppm) 104.39, 101.11, 93.29, 84.14, 78.12, 9.31, 5.41, 1.38, 1.26, −3.51, −5.29, −16.79, −33.17, −35.13, −39.40, −47.84. ATR-IR (cm^{-1}): 2961, 2924, 2868, 1520, 1457, 1430, 1394, 1372, 1322, 1249, 1014. Anal. Calcd. for $C_{42}H_{63}N_5Fe_2$ (%): C, 67.29; H, 8.47; N, 9.34. Found: C, 66.89; H, 8.57; N, 9.02. μ_{eff} = 5.4(2) μ_B.

$Fe_2(\mu$−κC:κN-HCN*t*Bu)(μ-H)L, 3-tBu. To a 20 mL scintillation vial charged with $Fe_2(\mu\text{-H})_2\mathbf{L}$ (150.0 mg, 220.0 μmol), 4.0 mL of PhMe, and a PTFE magnetic stir bar at ambient temperature was added *t*BuNC (27.5 mg, 330.0 μmol) dropwise dissolved in 2.0 mL of PhMe. The reaction mixture was stirred at ambient temperature for 3 h, after which the solvent was evaporated under reduced pressure, affording **3-tBu** as a dark red solid (134.7 mg, 80.2%). Single crystals for X-ray diffraction (XRD) diffraction were obtained as described for **2-iPr** (13.9 mg, 8.2%). ^{1}H NMR (400 MHz, C_6D_6, 298 K) δ (ppm): 94.17, 87.58, 74.81, 65.20, 9.56, 8.86, 4.64, 0.87, −2.77, −15.48, −27.86, −30.60. ATR-IR (cm^{-1}): 2961, 2924, 2868, 1520, 1457, 1430, 1394, 1372, 1322, 1249, 1014. Anal. Calcd. for $C_{43}H_{65}N_5Fe_2$ (%): C, 67.63; H, 8.58; N, 9.17. Found: C, 67.38; H, 8.69; N, 9.05. μ_{eff} = 5.6(2) μ_B.

$Fe_2(\mu$−κC:κN-HCNMe)(μ-H)L, 3-Me. A 20 mL scintillation vial was charged with $Fe_2(\mu\text{-H})_2\mathbf{L}$ (5.0 mg, 7.3 μmol), 4 mL of PhMe, and a Pyrex magnetic stir bar, and then cooled to −33 °C. To this solution was added MeNC (36.7 μL, 0.1 M in PhMe, 3.7 μmol) dropwise precooled to −33 °C. The reaction was stirred at −33 °C for 12 h and then at ambient temperature for 30 min. The reaction was then cooled to −33 °C, followed by dropwise addition of a second portion of MeNC (36.7 μL, 0.1 M in PhMe, 3.7 μmol). As before, the reaction was stirred at −33 °C for 12 h, and then for 30 min at ambient temperature. *NOTE: Sequential addition of 0.5 equiv of MeNC is required as addition of 1 equiv affords a mixture of the 1 and 2 equiv products, and unreacted $Fe_2(\mu\text{-H})_2$**L**.* All volatile species were removed under reduced pressure to yield a dark brown solid (4.9 mg, 6.8 μmol). Single crystals suitable for X-ray diffraction were obtained by slow evaporation from a saturated solution in diethyl ether at ambient temperature. ^{1}H NMR (400 MHz, C_6D_6, 298 K) δ (ppm): 96.25, 92.28, 90.40, 89.67, 81.62, 9.60, 2.11, 0.12, −3.17, −7.40, −16.55, −18.69, −34.54, −36.03. ATR-IR (cm^{-1}): 2959, 2927, 2869, 1527, 1459, 1428, 1398, 1372, 1329, 1019. Anal. Calcd. for $C_{40}H_{59}N_5Fe_2$·1 $C_4H_{10}O$ (%): C, 66.41; H, 8.74; N, 8.80. Found: C, 66.05; H, 8.48; N, 9.17. μ_{eff} = 4.2(2) μ_B.

https://doi.org/10.1021/acs.inorgchem.4c03256
Inorg. Chem. 2024, 63, 21083−21091

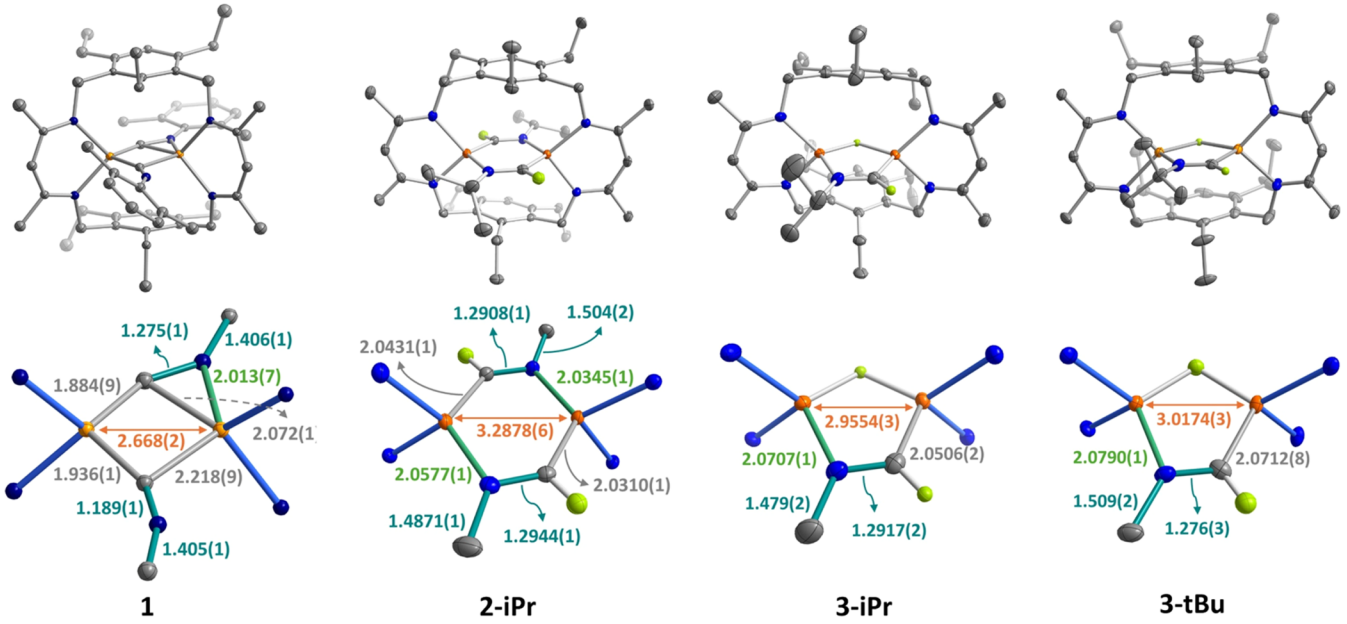

Figure 1. Crystal structures of **1-Xyl, 2-iPr, 3-iPr**, and **3-tBu** with thermal ellipsoids at 50% probability level from left to right, respectively (top). Solvent molecules and hydrogen atoms were removed for clarity. Primary coordination spheres of Fe ions in **1-Xyl, 2-iPr, 3-iPr**, and **3-tBu**, respectively, with pertinent bond lengths in Å (bottom). H, C, N, and Fe atoms are shown as green, gray, dark blue, and orange ellipsoids, respectively. The *t*-butyl group and one ethyl moiety in **3-tBu**, and one of the ethyl substituents and the one of the phenyl rings in **3-iPr** were positionally disordered; the depicted structures represent the models with ≥50% occupancy for the disordered fragment.

Reaction of $Fe_2(\mu\text{-}H)_2$L with 2 Equivalent of MeNC. This reaction was performed as described for the 1 equiv reaction above, except that MeNC was added in four separate portions (4 × 36.7 μL, 0.1 M in PhMe, 4 × 3.7 μmol). The dark, red-colored reaction mixture was then dried in vacuo to yield a dark brown solid (5.3 mg, 7.0 μmol). ^{1}H NMR (400 MHz, C_6D_6, 298 K) δ (ppm): 121.23, 119.63, 94.62, 84.95, 62.24, 20.71, 0.77, −0.57, −3.91, −7.14, −39.92, −43.64, −48.95, −51.32, −79.76. ATR-IR (cm^{-1}): 2958, 2923, 2867, 1512, 1459, 1427, 1394, 1371, 1319, 1015.

Reaction of $Fe_2(\mu\text{-}H)_2$L with 2 Equivalent of PhNC. $Fe_2(\mu\text{-}H)_2$L (53.7 mg, 78.9 μmol) was dissolved in 4.0 mL of PhMe. To the scintillation vial containing this mixture, a solution of PhNC (2.1350 mL, 77.58 mM in PhMe, 165.7 μmol) was added dropwise, resulting in a color change to reddish-brown upon mixing. The reaction was stirred for 90 min at ambient temperature, and then dried under reduced pressure to yield a brown solid (66.1 mg). ^{1}H NMR (400 MHz, C_6D_6, 298 K) δ (ppm): 90.24, 83.84, 69.16, 65.07, 16.55, 9.51, 4.26, 2.09, 1.16, 0.44, −2.10, −7.28, −27.40, −30.80. ATR-IR (cm^{-1}): 2959, 2925, 2867, 1592, 1518, 1458, 1429, 1393, 1372, 1322, 1018.

RESULTS AND DISCUSSION

Treating $Fe_2(\mu\text{-}H)_2$L with 2 equiv of 2,6-xylyl isocyanide (XylNC) in toluene at ambient temperature afforded a C_{2v} symmetric species, **1-Xyl**, and H_2 (δ = 4.50 ppm), based on ^{1}H NMR spectra of product mixture (Figures S1 and S4). IR spectra recorded on **1-Xyl** have strong absorptions at 1820 and 1853 cm^{-1}, consistent with bound RNC ligands (Figure S3).[34] A transient species was observed by NMR spectroscopy 10 min after the addition of XylNC at ambient temperature (Figure S5). Resonances for this transient disappear as the reaction proceeds, with those for **1-Xyl** concomitantly increasing in intensity, consistent with, but not confirmatory of, this transient as a reaction intermediate. Reaction of **1** with fewer equiv of XylNC results in unreacted $Fe_2(\mu\text{-}H)_2$L and **1-Xyl**. The solid-state structure of **1-Xyl** contains a diiron core with one isocyanide bound in a $\mu\text{-}\eta^1\text{:}\eta^2$ fashion and between the ligand arene rings, and a second isocyanide coordinated in a μ-1,1 mode (Figure 1). The observed solid-state C_s symmetry of **1-Xyl** differs from the solution-phase C_{2v} symmetry, implying that the isocyanide coordination modes are fluxional on the NMR time scale at ambient temperature or the observed asymmetry arises from crystal packing effects. The $\mu\text{-}\eta^1\text{:}\eta^2$-xylyl isocyanide N≡C bond length is longer as compared to that of the μ-1,1-isocyanide (viz. 1.275(1) vs 1.189(1) Å, respectively), as expected given the greater extent of formal sp^2 hybridization based on the C≡N−C_{xylyl} bond angle (viz. 138.4(9) vs 158.6(1)°, respectively).[22,35] Typically, the $\mu\text{-}\eta^1\text{:}\eta^2$ mode is observed for N_2 and isocyanides bound to reduced early transition metals and is rarely observed for late 3d metals, including the few examples of heterometallic dinuclear complexes of Fe and a 4d transition metal.[36−55] The only structurally characterized examples of a $\mu\text{-}\eta^1\text{:}\eta^2$-isocyanide in a homometallic dinuclear 3d metal complex are the dimanganese(0) and dititanium(III) complexes reported by Balch and Cloke, respectively.[56,57] A holistic comparison of the reported N≡C, M−η^2:C, and M−η^2:N bond distances and the assigned ν_{NC} energies and those for **1-Xyl** highlight that the bond metrics are poorly correlated with the IR data (Table S1). For example, the N≡C bond distance in $Mn_2(\mu\text{-}\eta^1\text{:}\eta^2\text{-}p\text{-}CH_3C_6H_4NC)(Ph_2PCH_2PPh_2)_2(CO)_4$ of 1.2479(2) Å is comparable to that in **1-Xyl**, yet the ν_{NC} is observed at 1661 vs 1820 cm^{-1} for **1-Xyl**.[56,57] Nonetheless, the trend that **1-Xyl** exhibits less activation of isocyanide agrees with the greater electronegativity of Fe vs metals in other reported examples and is consistent with IR data for a heterometallic dinuclear complex containing an η^2-isocyanide bound to an Fe center.[38] In contrast to the local pseudotetrahedral geometry (τ_4 = 0.72 and 0.85) at each iron center of **1-Xyl**, a previously reported mononuclear bis(isocyanide) Fe(I) β-diketiminate complex exhibits square planar geometry, likely a consequence of the geometric constraints afforded by the cyclophane ligand used here.[16] The mononuclear complex can also accommodate a

https://doi.org/10.1021/acs.inorgchem.4c03256
Inorg. Chem. 2024, 63, 21083−21091

third isocyanide donor to form a tris(isocyanide) Fe(I) complex, which is similar to the related polycarbonyl Fe(I) β-diketiminate complexes.[58] By contrast, NMR spectra of **1-Xyl** were unchanged upon the addition of excess XylNC, even with heating to 60 °C for 24 h.[59] Together with prior observations for the coordination of CO and N_2 to diiron complexes of this ligand, we conclude that the $\mathbf{L}^{2-}$ ligand effectively controls the coordination number and the local coordination geometry of each metal center within the complex.

We then reacted $Fe_2(\mu\text{-H})_2\mathbf{L}$ with 2 equiv of isopropyl isocyanide (iPrNC), which yielded a C_s symmetric product **2-iPr** lacking the IR absorptions in the 1700−2200 cm^{-1} range (Figures S6 and S8). In the solid-state structure of **2-iPr**, the insertion of an iPrNC into each μ-hydride affords the bis[$\mu-\kappa C:\kappa N$-(isopropyl)iminoformyl]diiron complex (Figure 1). Longer C−N bond lengths of 1.2908(1) and 1.2944(1) Å and more acute C−N−C_{iPr} bond angles (121.90(1) and 122.45(1)°) compared to those in **1-Xyl** support decreased CN bond order.[60−62] The nominally coplanar β-diketiminate arms in **2-iPr** with a dihedral angle between BDI planes of 172.951(1)° as compared to **1-Xyl** and to other complexes of $\mathbf{L}^{2-}$ reveal the flexibility of this cyclophane ligand to accommodate the steric demands of the iPr group.[24,63]

Formation of **2-iPr** is expected to be stepwise, traversing a (μ-hydrido)(μ-iminoformyl) complex. Then, reaction of $Fe_2(\mu\text{-H})_2\mathbf{L}$ with 1 equiv of *i*PrNC expectedly generated the (μ-hydrido)($\mu-\kappa C:\kappa N$-iminoformyl) diiron(II) complex, **3-iPr**, based on ^{1}H NMR, IR, and single-crystal X-ray diffraction (XRD) data (Figures 1, S9 and S11). From XRD data on single crystals of **3-iPr**, the iminoformyl bridges the Fe centers in a μ-1,2 mode and outside of the cyclophane arene cavity, consistent with the greater steric accessibility of this hydride as compared to the hydride within the ligand cavity (Figure 1). Addition of a second equivalent of *i*PrNC to **3-iPr** yielded **2-iPr**, corroborating the stepwise formation of **2-iPr** from $Fe_2(\mu\text{-H})_2\mathbf{L}$ (Figure S12). Ligand flexibility is again evident with substantial pinching of the cyclophane cavity—the arene−arene dihedral angle is 19.752(2)°—attributed to the relative differences in steric demands of hydride vs the (isopropyl)-iminoformyl (Figure S24).

To probe steric effects of the isocyanide substituent on the reaction, $Fe_2(\mu\text{-H})_2\mathbf{L}$ was treated with methyl- or phenyl isocyanide, which yielded product mixtures with ^{1}H NMR and IR spectra consistent with migratory insertion products (Figures S16−S18 and S20−S23). The crystal structure for the product of the reaction with 1 equiv of methyl isocyanide (MeNC), **3-Me**, evidences insertion of MeNC into the less accessible hydride within the cyclophane cavity, implying that the internal hydride is more reactive (Figure S19). Selective formation of **3-iPr** and **3-tBu** (vide infra) in which the isocyanide insertion is at the more accessible hydride indicates that the site of the reaction is finely balanced between steric demands of the ligand and substrate, and electronic factors. Insertion reactivity for PhNC as for the alkyl isocyanides implies that the steric consequences of the two *ortho*-methyl groups in XylNC preclude migratory insertion and lead to reductive elimination instead. Steric clashes from the two *ortho*-methyl groups in the xylyl group and the iminoformyl (if formed) would orient the iminoformyl out-of-plane with the xylyl ring, introducing steric conflicts between the ligand arene or Et groups.[64−71]

Similarly, reaction of $Fe_2(\mu\text{-H})_2\mathbf{L}$ with 1 equiv of *tert*-butyl isocyanide (*t*BuNC) at ambient temperature afforded **3-tBu**, the *tert*-butyl analogue of **3-iPr**, with comparable ^{1}H NMR, IR, and XRD data (Figures 1, S13, and S15). In contrast to the reaction of $Fe_2(\mu\text{-H})_2\mathbf{L}$ with iPrNC, reaction of either $Fe_2(\mu\text{-H})_2\mathbf{L}$ with more than 2 equiv of *t*BuNC or **3-tBu** with additional equivalent of *t*BuNC results only in **3-tBu**, even with heating to 60 °C for 1 d. We then conclude that the steric demands of the *t*Bu- group preclude migratory insertion of a second equivalent of *t*BuNC. A similar outcome was recently reported by Crimmin and co-workers for a tetrameric magnesium hydride cluster for which reaction with XylNC results in insertion into two of the Mg−(μ-H) bonds whereas MeNC inserted into all four hydride sites.[72] The XRD structure of **3-tBu** is isostructural with that of **3-iPr**, with comparable positions of the bridging iminoformyl outside of the cyclophane cavity (Figure 1). Electron density corresponding to the bridging hydride was evident in and could be readily modeled from the XRD data of **3-tBu**. The dihedral angle between the BDI arms in **3-tBu** and that in **3-iPr** (viz. 147.218(1) and 131.972(3)°, respectively), suggest that the steric demands of the *tert*-butyl group in **3-tBu** are relieved by an outward rotation of the BDI arms.

The observed steric effects can arise from a mechanism involving an initial associative step followed by either reductive elimination or migratory insertion. Therefore, we qualitatively evaluated the differences in the overall reaction rate as a function of the substituent. Assuming that the form of the rate laws for migratory insertion are substrate independent (i.e., same form for *t*BuNC and MeNC), we reacted solutions of $Fe_2(\mu\text{-H})_2\mathbf{L}$ (20.61 mM) and methyl-, isopropyl-, and *t*-butyl isocyanides (43.30 mM), and recorded NMR spectra at different time points at ambient temperature after mixing. In all cases, the first insertion was complete prior to the first recorded measurement at ∼10 min after mixing, with the complete consumption of $Fe_2(\mu\text{-H})_2\mathbf{L}$ (Figures S27−S29). However, a rate difference was observed for the second insertion with **2-iPr** requiring ∼48 min to completely convert to **3-iPr** whereas the double insertion reaction with MeNC was complete within 15 min (Figures S20−S21 and S28−S29).

The retained hydrides in the **3** series of complexes are presumed competent for migratory insertion given the conversion of **3-iPr** to **2-iPr**. However, we were keen to explore reaction with substrates for which insertion is unlikely. Treating **3-tBu** with XylNC at ambient temperature in a J-Young NMR tube with C_6D_6 as the solvent surprisingly yielded **1-Xyl** as the only observable paramagnetic product by ^{1}H NMR spectroscopy (Figure S30). To explore the fate of the iminoformyl ligand, we recorded ^{1}H NMR and mass spectra of the volatile species in this product mixture (Figures S31 and S32). Of the chemical shifts observed in the volatile species NMR spectrum, the resonances at δ = 1.14 and 3.79 ppm are consistent with 1,3,5-tri*tert*-butylhexahydro-1,3,5-triazine, which is one reported product of oligomerization of *tert*-butylaldimine.[73] ESI-HRMS(+) of the volatile products showed an ion envelope at m/z = 86.0969, as expected for *tert*-butylaldimine, *t*BuNCH_2 (Figure S31). The aldimine likely forms by the reductive elimination of iminoformyl and hydride ligands in **3-tBu** although such a transformation remains rare given the propensity of isocyanides to readily insert into metal−hydrogen and metal−carbon bonds.[17] However, the presence of other as yet unidentified volatile organic products suggests that other pathways are possible for the reaction of **3-**

https://doi.org/10.1021/acs.inorgchem.4c03256
Inorg. Chem. 2024, 63, 21083−21091

Scheme 3. Proposed Reaction Mechanism for the Reaction of Isocyanides with $Fe_2(\mu\text{-}H)_2L$

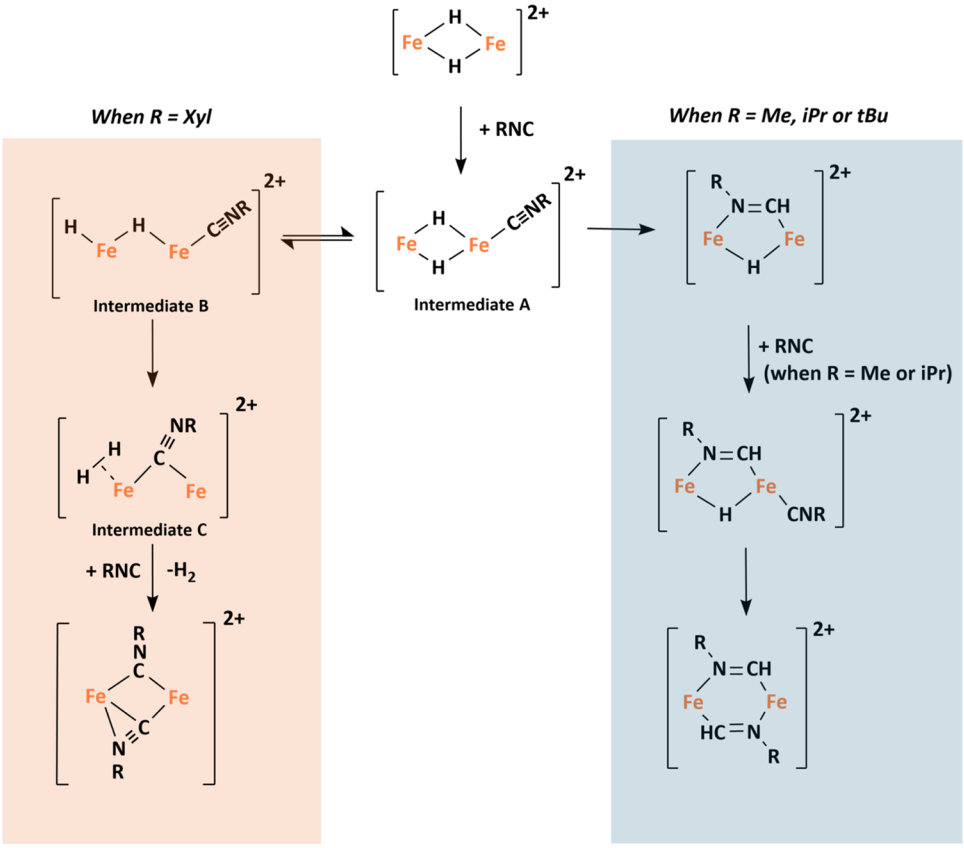

tBu with an isocyanide incapable of inserting into the Fe−(μ-H)−Fe bond.

Aware that detailed kinetic studies are needed to support an associative or dissociative mechanism for the reaction of isocyanides with $Fe_2(\mu\text{-}H)_2$**L**, the coordinatively unsaturated metal centers in $Fe_2(\mu\text{-}H)_2$**L** hint at an associative mechanism (Scheme 3). We cannot exclude an equilibrium between $Fe_2(\mu\text{-}H)_2$**L** and a Kubas complex, although work on a related system suggests such a Kubas complex must bind H_2 strongly or exhibit facile oxidative addition.[74] H_2 elimination is not also observed from $Fe_2(\mu\text{-}H)_2$**L** upon heating or ultraviolet (UV) irradiation (280 or 360 nm), suggesting reductive elimination is disfavored in the absence of the substrate.[75] Prior reactivity studies by our group on the related tri(μ-hydrido)triiron(II) cluster supported on a tris(β-diketiminate) cyclophane suggested that bridging hydrides can readily change coordination modes from μ^2 to semibridging, μ^3, or terminal.[74,76,77] Taken together, we propose an associative pathway wherein isocyanide coordination leads to isomerization of the hydride coordination modes (Intermediate A to Intermediate B). Binuclear reductive elimination is symmetry-forbidden, implying that isomerization is necessary to generate a terminal hydride competent for elimination.[78] We speculate that the transient species observed in NMR spectroscopy could be one of the structures corresponding to intermediates A−C, with the identity being dependent on the rates of isomerization, reductive elimination, and strength of the Fe−H_2 interaction. Prior work by Hong et al., on the related trinucleating cyclophane suggests that isomerization should be facile and the structure of Intermediate B is reminiscent of the N_2 bridged complex reported by Torres et al., supporting Intermediate B as a preferred assignment.[63] Where insertion is preferred over reductive elimination, migratory insertion may occur from intermediate A to directly access the iminoformyl product. An analogous second insertion, if sterically accessible, then affords bis(iminoformyl) complexes.

Our observations here of xylyl isocyanide resulting in H_2 elimination whereas other isocyanides undergoing migratory insertion to iminoformyl contrasts with Riera and co-workers' report (Scheme 1).[22] In that report, the steric demands of the ancillary ligand (i.e., phosphine donor) control reductive elimination versus migratory insertion, with a more sterically encumbered ancillary ligand yielding insertion products and a less encumbering ligand affording reductive elimination products.[22] Similar to our observations of substrate steric effects dictating the reaction outcome, Alt and co-workers reported that reaction of a di(hydrido)ditungsten complex with *t*BuNC results in H_2 reductive elimination whereas treatment with MeNC gives a 1,2-insertion product (Scheme 1).[23] The discrimination for elimination observed here, however, is reserved only to xylyl isocyanide, and may arise from the unique steric conflicts imposed by the two *ortho*-methyl groups, whereas steric bulk of the isonitrile substituent correlates with whether one or both hydrides are competent for insertion.[79]

The semihydrogenation of *t*BuNC to *t*BuNCH_2 by a diiron dihydride cluster is reminiscent of the products from reduction of MeCN by the molybdenum-dependent nitrogenase.[10] Contrastingly, the proposed reaction pathway for the nitrogenase cofactor traverses an aminocarbene transient vs the iminoformyl observed here. To our knowledge, aldimine reductive eliminations are exceedingly rare and only observed

https://doi.org/10.1021/acs.inorgchem.4c03256
Inorg. Chem. 2024, 63, 21083−21091

for late 3d metal hydrides. The prior report from Figueroa and co-workers results from the steric crowding at the metal center because of the sterically demanding terphenyl isocyanides.[12] Ligand steric conflicts here are manifested by the cavity shape and size, with the former limiting the rotation of the xylyl group needed for migratory insertion and the latter controlling the extent of insertion (i.e., one vs two hydrides). With respect to aldimine elimination then, coordination of the π-acidic xylyl isocyanide electronically primes the metal centers for reductive elimination, likely proceeding by a mechanism involving cluster core reorganization similar to the proposed isomerization of Intermediate A to Intermediate B. Similar structural changes to the local environment of the iron centers have been previously noted in dinitrogen and CO coordination to related complexes.[24,63,76]

CONCLUSIONS

Reaction of a low-coordinate di(μ-hydrido)diiron(II) complex, $Fe_2(\mu\text{-}H)_2\mathbf{L}$, with various isocyanides leads to reductive elimination of H_2 for XylNC or migratory insertion for all other isocyanides tested. Migratory insertion can be arrested by either the control of reaction equivalents or by the steric demands of the isocyanide substituent. Analogous to the elimination of H_2 from $Fe_2(\mu\text{-}H)_2\mathbf{L}$ when treated with CO or XylNC, the reductive elimination of *tert*-butylaldimine is also accessible for this system. The reactivity of the monohydride complexes reported here as well as other transformations involving isocyanides are currently under investigation.

ASSOCIATED CONTENT

Supporting Information

The Supporting Information is available free of charge at https://pubs.acs.org/doi/10.1021/acs.inorgchem.4c03256.

^{1}H NMR; IR; ESI(+)/HRMS; and crystal data tables (PDF)

Accession Codes

CCDC 2353888−2353890, 2353893, and 2353894 contain the supplementary crystallographic data for this paper. These data can be obtained free of charge via www.ccdc.cam.ac.uk/data_request/cif, or by emailing data_request@ccdc.cam.ac.uk, or by contacting The Cambridge Crystallographic Data Centre, 12 Union Road, Cambridge CB2 1EZ, UK; fax: +44 1223 336033.

AUTHOR INFORMATION

Corresponding Author

Leslie J. Murray − *Center for Catalysis and Florida Center for Heterocyclic Chemistry, Department of Chemistry, University of Florida, Gainesville, Florida 32611, United States;* orcid.org/0000-0002-1568-958X; Email: murray@chem.ufl.edu

Authors

Titto Sunil John − *Center for Catalysis and Florida Center for Heterocyclic Chemistry, Department of Chemistry, University of Florida, Gainesville, Florida 32611, United States;* orcid.org/0000-0002-6100-4262

Łukasz Dobrzycki − *Department of Chemistry, University of Florida, Gainesville, Florida 32611, United States*

Vincent J. Catalano − *Department of Chemistry, University of Nevada, Reno, Nevada 89557, United States;* orcid.org/0000-0003-2151-2892

Complete contact information is available at: https://pubs.acs.org/10.1021/acs.inorgchem.4c03256

Author Contributions

The manuscript was written through contributions of all authors. All authors have given approval to the final version of the manuscript.

Funding

T.S.J. and L.J.M. acknowledge funding from the National Science Foundation (CHE-2102098). X-ray diffractometers for measurements at the Center for X-ray Crystallography at UF were supported by the National Science Foundation (CHE-1828064). Mass spectrometry data were collected on instrumentation supported by the National Institutes of Health (S10 OD021758-01A1 and S10 OD030250-01A1).

Notes

The authors declare no competing financial interest.

ACKNOWLEDGMENTS

The authors acknowledge Dr. S. MacMillan for XRD data collection of **1-Xyl**, **2-iPr**, and **3-tBu**.

REFERENCES

(1) Rofer-DePoorter, C. K. A Comprehensive Mechanism for the Fischer−Tropsch Synthesis. *Chem. Rev.* **1981**, *81* (5), 447−474.

(2) Ertl, G. Primary Steps in Catalytic Synthesis of Ammonia. *J. Vac. Sci. Technol., A* **1983**, *1* (2), 1247−1253.

(3) De Smit, E.; Weckhuysen, B. M. The Renaissance of Iron-Based Fischer−Tropsch Synthesis: On the Multifaceted Catalyst Deactivation Behaviour. *Chem. Soc. Rev.* **2008**, *37* (12), 2758−2781.

(4) Seefeldt, L. C.; Yang, Z.-Y.; Lukoyanov, D. A.; Harris, D. F.; Dean, D. R.; Raugei, S.; Hoffman, B. M. Reduction of Substrates by Nitrogenases. *Chem. Rev.* **2020**, *120* (12), 5082−5106.

(5) Hoffman, B. M.; Lukoyanov, D.; Yang, Z.-Y.; Dean, D. R.; Seefeldt, L. C. Mechanism of Nitrogen Fixation by Nitrogenase: The Next Stage. *Chem. Rev.* **2014**, *114* (8), 4041−4062.

(6) Adamska, A.; Silakov, A.; Lambertz, C.; Rüdiger, O.; Happe, T.; Reijerse, E.; Lubitz, W. Identification and Characterization of the "Super-Reduced" State of the H-Cluster in [FeFe] Hydrogenase: A New Building Block for the Catalytic Cycle? *Angew. Chem., Int. Ed.* **2012**, *51* (46), 11458−11462.

(7) Shima, T.; Zhuo, Q.; Hou, Z. Dinitrogen Activation and Transformation by Multimetallic Polyhydride Complexes. *Coord. Chem. Rev.* **2022**, *472*, No. 214766.

(8) Ballmann, J.; Munhá, R. F.; Fryzuk, M. D. The Hydride Route to the Preparation of Dinitrogen Complexes. *Chem. Commun.* **2010**, *46* (7), 1013−1025.

(9) Carpenter, A. E.; Mokhtarzadeh, C. C.; Ripatti, D. S.; Havrylyuk, I.; Kamezawa, R.; Moore, C. E.; Rheingold, A. L.; Figueroa, J. S. Comparative Measure of the Electronic Influence of Highly Substituted Aryl Isocyanides. *Inorg. Chem.* **2015**, *54* (6), 2936−2944.

(10) Rubinson, J. F.; Corbin, J. L.; Burgess, B. K. Nitrogenase Reactivity: Methyl Isocyanide as Substrate and Inhibitor. *Biochemistry* **1983**, *22* (26), 6260−6268.

(11) Ionkin, A.; Solek, S.; Bryndza, H.; Koch, T. Isonitriles in Fischer−Tropsch Catalysis. *Catal. Lett.* **1999**, *61* (3−4), 139−141.

(12) Carpenter, A. E.; Rheingold, A. L.; Figueroa, J. S. A Well-Defined Isocyano Analogue of HCo(CO)4. 1: Synthesis, Decomposition, and Catalytic 1,1-Hydrogenation of Isocyanides. *Organometallics* **2016**, *35* (14), 2309−2318.

(13) Salsi, F.; Hagenbach, A.; Figueroa, J. S.; Abram, U. Na[Tc(CO)(CN p -F-Ar DArF2) 4]: An Isocyanide Analogue of the Elusive Na[Tc(CO) 5]. *Chem. Commun.* **2023**, *59* (27), 4028−4031.

(14) Agnew, D. W.; Moore, C. E.; Rheingold, A. L.; Figueroa, J. S. Kinetic Destabilization of Metal−Metal Single Bonds: Isolation of a

Pentacoordinate Manganese(0) Monoradical. *Angew. Chem., Int. Ed.* **2015**, *54* (43), 12673−12677.
(15) Zhuo, Q.; Yang, J.; Zhou, X.; Shima, T.; Luo, Y.; Hou, Z. Dinitrogen Cleavage and Multicoupling with Isocyanides in a Dititanium Dihydride Framework. *J. Am. Chem. Soc.* **2024**, *146* (15), 10984−10992.
(16) Yu, Y.; Sadique, A. R.; Smith, J. M.; Dugan, T. R.; Cowley, R. E.; Brennessel, W. W.; Flaschenriem, C. J.; Bill, E.; Cundari, T. R.; Holland, P. L. The Reactivity Patterns of Low-Coordinate Iron-Hydride Complexes. *J. Am. Chem. Soc.* **2008**, *130* (20), 6624−6638.
(17) Boyarskiy, V. P.; Bokach, N. A.; Luzyanin, K. V.; Kukushkin, V. Y. Metal-Mediated and Metal-Catalyzed Reactions of Isocyanides. *Chem. Rev.* **2015**, *115* (7), 2698−2779.
(18) Collet, J. W.; Roose, T. R.; Ruijter, E.; Maes, B. U. W.; Orru, R. V. A. Base Metal Catalyzed Isocyanide Insertions. *Angew. Chem., Int. Ed.* **2020**, *59* (2), 540−558.
(19) Beringhelli, T.; D'Alfonso, G.; Minoja, A.; Ciani, G.; Moret, M.; Sironi, A. Insertion of Isocyanides into Metal-Hydrogen Bonds in Triangular Hydrido-Carbonyl Clusters of Rhenium. X-Ray Crystal Structures of [Re3(μ-H)3(μ-H2-CHNR)(CO)10]− (R = p-Tolyl) and of [Re3(μ-H)3(M3-H2-CHNR)(CO)9]− (R = Cyclohexyl). *Organometallics* **1991**, *10* (9), 3131−3138.
(20) Alvarez, M. A.; García, M. E.; García-Vivó, D.; Ruiz, M. A.; Vega, M. F. Insertion, Rearrangement, and Coupling Processes in the Reactions of the Unsaturated Hydride Complex [W2(H5-C5H5)2(H)(μ-PCy2)(CO)2] with Isocyanides. *Organometallics* **2013**, *32* (16), 4543−4555.
(21) Anslyn, E. V.; Green, M.; Nicola, G.; Rosenberg, E. Mechanistic Studies on Metal to Ligand Hydrogen Transfer in the Thermal Reactions of H(μ-H)Os3(CO)10(CNR): Evidence for Proton Barrier Tunneling in a Metal to Ligand Hydrogen Transfer. *Organometallics* **1991**, *10* (8), 2600−2605.
(22) Alonso, F. J. G.; Sanz, M. G.; Riera, V.; Abril, A. A.; Tiripicchio, A.; Ugozzoli, F. Reactions of Unsaturated Dihydrido Carbonyl Complexes of Manganese(I) with Nitriles and Isonitriles. Preparation and Characterization of the First Binuclear μ,H1,H2-NCR Derivatives. *Organometallics* **1992**, *11* (2), 801−808.
(23) Alt, H. G.; Frister, T. Darstellung Eines Dimetallacyclopropen-Komplexes Durch Insertion von Methylisonitril in Eine W—H—W-Brücke. *J. Organomet. Chem.* **1985**, *293* (1), C7−C9.
(24) Singh, D.; Knight, B. J.; Catalano, V. J.; García-Serres, R.; Maurel, V.; Mouesca, J.-M.; Murray, L. J. Partial Deoxygenative CO Homocoupling by a Diiron Complex. *Angew. Chem., Int. Ed.* **2023**, *62* (41), No. e202308813.
(25) Schuster, R. E.; Scott, J. E.; Casanova, J., Jr. Methyl Isocyanide. *Org. Synth.* **2003**, 75.
(26) *CrysAlisPro*; Rigaku OD: The Woodlands, TX, 2015.
(27) Sheldrick, G. M. A Short History of SHELX. *Acta Crystallogr., Sect. A: Found. Crystallogr.* **2008**, *64* (1), 112−122.
(28) Sheldrick, G. M. SHELXT—Integrated Space-Group and Crystal-Structure Determination. *Acta Crystallogr., Sect. A: Found. Adv.* **2015**, *71* (1), 3−8.
(29) Müller, P. Practical Suggestions for Better Crystal Structures. *Crystallogr. Revi.* **2009**, *15* (1), 57−83.
(30) Bruker Nano, Inc.. *APEX3 V2019* 2019.
(31) Bruker Nano, Inc.. *SAINT V8.40A*, 2019.
(32) Bruker Nano, Inc.. *SADABS V2016/2*, 2019.
(33) Sheldrick, G. M. Crystal Structure Refinement with SHELXL. *Acta Crystallogr., Sect. C: Struct. Chem.* **2015**, *71* (1), 3−8.
(34) Singleton, E.; Oosthuizen, H. E. Metal Isocyanide Complexes. *Adv. Organomet. Chem.* **1983**, *22*, 209−310.
(35) Chisholm, M. H.; Cotton, F. A.; Extine, M. W.; Rankel, L. A. Reactions of Metal-to-Metal Multiple Bonds. 2. Reactions of Bis(Cyclopentadienyl)Tetracarbonyldimolybdenum with Small Unsaturated Molecules. Structural Characterization of.Mu.-Dimethylaminocyanamide-Bis(Cyclopentadienyl)Tetracarbonyldimolybdenum. *J. Am. Chem. Soc.* **1978**, *100* (3), 807−811.
(36) Gade, L. H.; Schubart, M.; Findeis, B.; Fabre, S.; Bezougli, I.; Lutz, M.; Scowen, I. J.; McPartlin, M. Synthesis and Reactivity of Early−Late Heterodinuclear Complexes Stabilized by a Trisilylsilane-Based Tripodal Amido Ligand. *Inorg. Chem.* **1999**, *38* (23), 5282−5294.
(37) Friedrich, S.; Gade, L. H.; Scowen, I. J.; McPartlin, M. A. Chelate-Amidozirconium Fragment as Building Block for Unsupported Trinuclear ZrM2 Heterobimetallic Complexes (M = Fe, Ru, Co). *Angew. Chem., Int. Ed.* **1996**, *35* (12), 1338−1341.
(38) Ohki, Y.; Araki, Y.; Tada, M.; Sakai, Y. Synthesis and Characterization of Bioinspired [Mo2Fe2]−Hydride Cluster Complexes and Their Application in the Catalytic Silylation of N2. *Chem. - Eur. J.* **2017**, *23* (53), 13240−13248.
(39) Bernal, I.; Brunner, H.; Wachter, J. Crystal and Molecular Structure of Triclinic [C5H5(CO)2Mol2(μ,H2-C≡NC6H5) and Comparison with Its Monoclinic Form. *J. Organomet. Chem.* **1984**, *277* (3), 395−401.
(40) Brunner, H.; Buchner, H.; Wachter, J.; Bernal, I.; Ries, W. H. Reactivity of the Metal—metal-Multiple Bond in Metal Carbonyl Derivatives: VI. Investigation into the Reaction of [C5Me5(CO)-2Mo]2 with CH3N═C═S: Formation and Crystal Structure of (C5Me5)2(CO)4Mo2(μ,H2-C≡NCH3). *J. Organomet. Chem.* **1983**, *244* (3), 247−255.
(41) Li, Q.; Luo, C.; Song, L. Reactions of Cyclohexyl Isocyanide with H5-Substituted Cyclo-Pentadienyl Mo−Mo Triply Bonded Complexes. Crystal Structure of [Mo(CO)2(H5-C5H4CO2CH3)]-2(μ-H2-CNC6H11). *Chin. J. Chem.* **2009**, *27* (9), 1711−1715.
(42) Bernal, I.; Draux, M.; Brunner, H.; Hoffmann, B.; Wachter, J. Reaction of (C5H5)2Mo2(CO)4 with Carbodiimides: Structural Characterization of C5H5(CO)2Mo(CNPh)Mo(NPh)C5H5, a Novel Complex Containing a Terminal Phenylimido and a Bridging Phenyl Isocyanide Ligand, and Its Reaction with P(OMe)31. *Organometallics* **1986**, *5* (2), 655−660.
(43) Adams, H.; Bailey, N. A.; Bannister, C.; Faers, M. A.; Fedorko, P.; Osborn, V. A.; Winter, M. J. The Addition of Isonitriles to [{M(CO)2(η-C5H5)}2] (M = Mo or W). Syntheses and Properties of [M2(μ-H2-CNR)(CO)4(η-C 5H5)2] (M = Mo or W, R = Me or But) and [{Mo(CNR)(CO)2(η-C5H5)}2] (R = Me or But). *J. Chem. Soc., Dalton Trans.* **1987**, *2*, 341−348.
(44) Herrmann, W. A.; Menjon, B.; Herdtweck, E. Chemistry of Oxophilic Transition Metals. 4. Reactivity of the Organozirconium(III) Complex (.Mu.-.Eta.5:.Eta.5-C10H8)[(.Mu.-Cl)Zr(.Eta.5-C5H5)]2 with Diphenyldiazomethane, Tert-Butyl Isocyanide, and Trimethylsilyl Azide: Diazo, Cyano, and Imido Complexes. *Organometallics* **1991**, *10* (7), 2134−2141.
(45) Alvarez, M. A.; Amor, I.; García, M. E.; García-Vivó, D.; Ruiz, M. A.; Sáez, D.; Hamidov, H.; Jeffery, J. C. Activity of Mo−Mo and Mo−P Multiple Bonds at the Phosphinidene Complex [Mo2Cp2{μ-P(2,4,6-C6H2tBu3)}(μ-CO)2] in Reactions with Isocyanides and Phosphine Ligands. *Inorg. Chim. Acta* **2015**, *424*, 103−115.
(46) Cuenca, T.; Gomez, R.; Gomez-Sal, P.; Rodriguez, G. M.; Royo, P. Reactions of Titanium- and Zirconium(III) Complexes with Unsaturated Organic Systems. X-Ray Structure of {[(.Eta.5-C5H5)-Zr(CH3)]2[.Mu.-.Eta.1-.Eta.2-CN(Me2C6H3)] (.Mu.-.Eta.5-.Eta.5-C10H8)}. *Organometallics* **1992**, *11* (3), 1229−1234.
(47) Li, B.; Xu, S.; Song, H.; Wang, B. Reactions of (Me2C)-(Me2Si)[(H5-C5H3)Mo(CO)3]2 with Nitrile and Subsequent Cleavage of the CN Bond by Cooperation of Molybdenum and Ruthenium. *J. Organomet. Chem.* **2008**, *693* (1), 87−96.
(48) Riera, V.; Ruiz, M. A.; Villafañe, F.; Bois, C.; Jeannin, Y. Synthesis, Crystal Structure and Heterometallic Derivatives of [Mo2Cp2(μ-σ,π-CNtBu)(PPh2CH2PPh2-P)(CO)3] (tBu = C-(CH3)3, Cp = η-C5H5). *J. Organomet. Chem.* **1990**, *382* (3), 407−417.
(49) Caselli, A.; Solari, E.; Scopelliti, R.; Floriani, C. A Synthetic Methodology to Niobium Alkylidenes: Reactivity of a NbNb Double Bond Anchored to a Calix[4]Arene Oxo Surface with Ketones, Aldehydes, Imines, and Isocyanides. *J. Am. Chem. Soc.* **1999**, *121* (36), 8296−8305.

https://doi.org/10.1021/acs.inorgchem.4c03256
Inorg. Chem. 2024, 63, 21083−21091

(50) Yeo, A.; Shaver, M. P.; Fryzuk, M. D. A. New Side-on End-On Ditantalum Dinitrogen Complex and Its Reaction with BuSiH3. *Z. Anorg. Allg. Chem.* **2015**, *641* (1), 123−127.
(51) Fryzuk, M. D.; Johnson, S. A.; Rettig, S. J. New Mode of Coordination for the Dinitrogen Ligand: A Dinuclear Tantalum Complex with a Bridging N2 Unit That Is Both Side-On and End-On. *J. Am. Chem. Soc.* **1998**, *120* (42), 11024−11025.
(52) Pun, D.; Lobkovsky, E.; Chirik, P. J. Indenyl Zirconium Dinitrogen Chemistry: N2 Coordination to an Isolated Zirconium Sandwich and Synthesis of Side-on, End-on Dinitrogen Compounds. *J. Am. Chem. Soc.* **2008**, *130* (18), 6047−6054.
(53) Fryzuk, M. D.; Johnson, S. A.; Patrick, B. O.; Albinati, A.; Mason, S. A.; Koetzle, T. F. New Mode of Coordination for the Dinitrogen Ligand: Formation, Bonding, and Reactivity of a Tantalum Complex with a Bridging N2 Unit That Is Both Side-On and End-On. *J. Am. Chem. Soc.* **2001**, *123* (17), 3960−3973.
(54) Wang, B.; Luo, G.; Nishiura, M.; Hu, S.; Shima, T.; Luo, Y.; Hou, Z. Dinitrogen Activation by Dihydrogen and a PNP-Ligated Titanium Complex. *J. Am. Chem. Soc.* **2017**, *139* (5), 1818−1821.
(55) Mo, Z.; Shima, T.; Hou, Z. Synthesis and Diverse Transformations of a Dinitrogen Dititanium Hydride Complex Bearing Rigid Acridane-Based PNP-Pincer Ligands. *Angew. Chem., Int. Ed.* **2020**, *59* (22), 8635−8644.
(56) Kilpatrick, A. F. R.; Green, J. C.; Cloke, F. G. N. Reactivity of a Dititanium Bis(Pentalene) Complex toward Heteroallenes and Main-Group Element−Element Bonds. *Organometallics* **2017**, *36* (2), 352−362.
(57) Benner, L. S.; Olmstead, M. M.; Balch, A. L. Structural Characterization of a Four-Electron Donating, Doubly-Bridging Isocyanide in (μ-*p*-CH3C6H4NC)Mn2(Ph2PCH2PPh2)2(CO)4. *J. Organomet. Chem.* **1978**, *159* (3), 289−298.
(58) Smith, J. M.; Sadique, A. R.; Cundari, T. R.; Rodgers, K. R.; Lukat-Rodgers, G.; Lachicotte, R. J.; Flaschenriem, C. J.; Vela, J.; Holland, P. L. Studies of Low-Coordinate Iron Dinitrogen Complexes. *J. Am. Chem. Soc.* **2006**, *128* (3), 756−769.
(59) Cowley, R. E.; Golder, M. R.; Eckert, N. A.; Al-Afyouni, M. H.; Holland, P. L. Mechanism of Catalytic Nitrene Transfer Using Iron(I)-Isocyanide Complexes. *Organometallics* **2013**, *32* (19), 5289−5298.
(60) Adams, R. D.; Dawoodi, Z. Importance of Trinuclear Coordination in the Activation and Desulfurization of a Thioformamido Ligand by a Triosmium Cluster. *J. Am. Chem. Soc.* **1981**, *103* (21), 6510−6512.
(61) Adams, R. D.; Dawoodi, Z.; Foust, D. F. Role of Heteroatoms in the Formation of Higher Nuclearity Transition-Metal Carbonyl Cluster Compounds. The Condensation of Small Clusters. *Organometallics* **1982**, *1* (2), 411−413.
(62) Dieck, H. T.; Klaus, J.; Kopf, J. A Novel Type of Diazadiene Co-Ordination Behaviour. X-Ray Structure of a Rhodium Complex with Bridging Azomethine Groups. *J. Chem. Soc., Chem. Commun.* **1982**, *11*, 574−575.
(63) Torres, J. F.; Oi, C. H.; Moseley, I. P.; El-Sakkout, N.; Knight, B. J.; Shearer, J.; García-Serres, R.; Zadrozny, J. M.; Murray, L. J. Dinitrogen Coordination to a High-Spin Diiron(I/II) Species. *Angew. Chem., Int. Ed.* **2022**, *61* (22), No. e202202329.
(64) Bhattacharya, S.; Saha, B. K. Inclusion of a Chiral Guest in a Centrosymmetric Organic Host Lattice. *CrystEngComm* **2011**, *13* (23), 6941−6944.
(65) Blair, A. D.; Hendsbee, A. D.; Masuda, J. D. 1-(2,4,6-Triisopropylphenyl)Ethanone. *Acta Crystallogr., Sect. E: Struct. Rep. Online* **2011**, *67* (10), No. o2731.
(66) Schowtka, B.; Müller, C.; Görls, H.; Westerhausen, M. Synthesis, Structures, and Spectroscopic Properties of 3-Aryl-5-(2-Pyridyl)Pyrazoles and Related Pyrazoles. *Z. Anorg. Allg. Chem.* **2014**, *640* (5), 916−925.
(67) Ito, Y.; Takahashi, H.; Hasegawa, J.; Turro, N. J. Photocyclization of 2,4,6-Triethylbenzophenones in the Solid State. *Tetrahedron* **2009**, *65* (3), 677−689.
(68) Takahashi, H.; Ito, Y. Low-Temperature-Induced Reversible Single-Crystal-to-Single-Crystal Phase Transition of 3,4-Dichloro-2′,4′,6′-Triethylbenzophenone. *CrystEngComm* **2010**, *12* (5), 1628−1634.
(69) Fukushima, S.; Ito, Y.; Hosomi, H.; Ohba, S. Structures and Photoreactivities of 2,4,6-Triisopropylbenzophenones. *Acta Crystallog. Section B: Struct. Sci.* **1998**, *54* (6), 895−906.
(70) Bąkowicz, J.; Skarżewski, J.; Turowska-Tyrk, I. Photo-Induced Structural Changes in Two Crystal Forms with Different Numbers of Independent Molecules. *CrystEngComm* **2011**, *13* (13), 4332−4338.
(71) Chen, C.; Bellows, S. M.; Holland, P. L. Tuning Steric and Electronic Effects in Transition-Metal β-Diketiminate Complexes. *Dalton Trans.* **2015**, *44* (38), 16654−16670.
(72) Yang, W.; White, A. J. P.; Crimmin, M. R. Cross-Coupling of CO and an Isocyanide Mediated by a Tetrameric Magnesium Hydride Cluster. *Chem. Sci.* **2024**, *15*, 11807−11813.
(73) Achternbosch, M.; Brieger, L.; Strohmann, C. Influence Of Lithium Coordinating Additives On The Structure Of Phenyldimethylsilyllithium. *Z. Anorg. Allg. Chem.* **2021**, *647* (9), 979−983.
(74) Anderton, K. J.; Knight, B. J.; Rheingold, A. L.; Abboud, K. A.; García-Serres, R.; Murray, L. J. Reactivity of Hydride Bridges in a High-Spin $[Fe_3(\mu\text{-}H)_3]^{3+}$ Cluster: Reversible H_2/CO Exchange and Fe−H/B−F Bond Metathesis. *Chem. Sci.* **2017**, *8* (5), 4123−4129.
(75) Kubas, G. J. Fundamentals of H2 Binding and Reactivity on Transition Metals Underlying Hydrogenase Function and H2 Production and Storage. *Chem. Rev.* **2007**, *107* (10), 4152−4205.
(76) Hong, D. H.; Ferreira, R. B.; Catalano, V. J.; García-Serres, R.; Shearer, J.; Murray, L. J. Access to Metal Centers and Fluxional Hydride Coordination Integral for CO2 Insertion into [Fe3(μ-H)3]3+ Clusters. *Inorg. Chem.* **2021**, *60* (10), 7228−7239.
(77) Hong, D. H.; Murray, L. J. Carbon Dioxide Insertion into Bridging Iron Hydrides: Kinetic and Mechanistic Studies. *Eur. J. Inorg. Chem.* **2019**, *2019* (15), 2146−2153.
(78) Trinquier, G.; Hoffmann, R. Dinuclear Reductive Eliminations. *Organometallics* **1984**, *3* (3), 370−380.
(79) Pombeiro, A. J. L.; da Silva, M. F. C. G.; Michelin, R. A. Aminocarbyne Complexes Derived from Isocyanides Activated towards Electrophilic Addition. *Coord. Chem. Rev.* **2001**, *218*, 43−74.

https://doi.org/10.1021/acs.inorgchem.4c03256
Inorg. Chem. 2024, 63, 21083−21091